Optical properties of Ag- and AgI-doped Ge–Ga–Te far-infrared chalcogenide glasses

Ci Cheng[1], Xunsi Wang[1*], Tiefeng Xu[1], Lihong Sun[1], Zhanghao Pan[1], Shuo Liu[1], Qingde Zhu[1], Fangxing Liao[1], Qiuhua Nie[1], Shixun Dai[1], Xiang Shen[1], Xianghua Zhang[2], Wei Chen[3*]

([1]*Laboratory of Infrared Material and Devices, The Research Institute of Advanced Technologies, Ningbo University, Ningbo, Zhejiang 315211, China*)

([2]*Laboratory of Glasses and Ceramics, UMR 6226 CNRS-University of Rennes 1, Rennes Cedex 135042, France*)

([3]*Department of Electrical Engineering, Shaoyang University, Shaoyang, Hunan 422004, China)*

Abstract: Te-based glasses are ideal material for life detection and infrared-sensing applications because of their excellent far-infrared properties. In this study, the influence of Ag- and AgI-doped Te-based glasses were discussed. Thermal and optical properties of the prepared glasses were evaluated using X-ray diffraction, differential scanning calorimetry, and Fourier transform infrared spectroscopy. Results show that these glass samples have good amorphous state and thermal stability. However, Ge–Ga–Te–Ag and Ge–Ga–Te–AgI glass systems exhibit completely different in optical properties. With an increase of Ag content, the absorption cut-off edge of Ge–Ga–Te–Ag glass system has a red shift. On the contrary, a blue shift appears in Ge–Ga–Te–AgI glass system with an increase of AgI content. Moreover, the transmittance of Ge–Ga–Te–Ag glass system deteriorates while that of Ge–Ga–Te–AgI glass system ameliorates. All glass samples have wide infrared transmission windows and the far-infrared cut-off wavelengths of these glasses are beyond 25 μm. The main absorption peaks of these glasses are eliminated through a purifying method.

Keywords: far-infrared; Te-based glasses; thermal stability; infrared transmission windows

1. Introduction

Chalcogenide glasses have unique advantages in infrared (IR) applications, especially in far-IR [1-11]. The far-IR cut-off wavelength of Te glass is usually greater than 20 μm. However, most Te glasses are unstable against crystallization because of strong metallic properties of Te atoms. Some electron-deficient additives, such as Ge, Ga, and I atoms, are doped into glass to improve the thermal stability and optical properties of Te-based chalcogenide glasses. Zhang et al. [1] proposed that elemental halogen doped into glass can open up the original network structure and improve the ability of glass formation. Nevertheless, the weak mechanical and low thermal characteristics of Te–X (Cl, Br, I) glasses limit the glasses to be fabricated as fibers or shaped into lenses. To overcome these limitations, many scientists exerted their efforts to develop suitable Te-based glasses. Wilhelm et al. [5] reported that Ge–Te–I ternary glass system has good thermal stability and wide IR transparency window, but elemental I can volatilize easily during the fiber fabrication. Maurugeon et al. [12] revealed that Ge–Te–Se chalcogenide glasses have good glass-forming ability and high IR transmission. However, the IR cut-off edge is limited by Se atoms. Danto et al. [3] reported that the IR cut-off edge of Ge–Ga–Te glass system is beyond 25 μm, but the IR transmission spectrum has an obvious absorption band. Ramesh et al. [13] reported

* Corresponding author. Fax: +86 574 87600947.

E-mail address: xunsiwang@siom.ac.cn (X.Wang).

that metal can improve connectivity of glass and stabilize glass structure. Recently, Sun et al. [14] proposed that halide can improve the abilities of glass formation and anti-crystallization. To date, comprehensive study about the different influence of Ag- and AgI-doped Ge–Ga–Te glasses has not been reported.

In our study, Ge–Ga–Te–Ag and Ge–Ga–Te–AgI glass samples were prepared by traditional melt-quenching method. This work aims to analyze different optical properties of two kinds of glass systems. This is the first comprehensive study to discuss the optical properties of metal- and metal halide-doped Te-based glasses. Thermal and optical properties were tested by differential scanning calorimetry (DSC) and Fourier transform IR spectroscopy (FTIR).

2. Experimental

For this experiment, $(Ge_{15}Ga_{10}Te_{75})_{100-x}(Ag)_x$ (x = 10, 20, 30, 40) glasses (named GGT–Ag10, GGT–Ag20, GGT–Ag30, and GGT–Ag40, respectively) and $(Ge_{15}Ga_{10}Te_{75})_{100-x}(AgI)_x$ (x= 10, 20, 30, 40) glasses (named GGT–AgI10, GGT–AgI20, GGT–AgI30, and GGT–AgI40, respectively) were prepared and investigated. Appropriate amounts of raw materials Ge, Ga, Te, Ag, and AgI with high purity were weighed carefully and transferred into quartz ampoules. The ampoules were sealed under vacuum (~10^{-3} Pa) and melted in a rocking furnace at 850 °C for 15 h to homogenize the mixtures. The ampoules were then swiftly quenched in ice water and annealed at 10 °C below glass transition temperature (T_g) for 5 h in several prepared furnaces to eliminate inner stress of glasses. Finally, glass samples were cut into discs and polished for testing.

The amorphous nature of glass samples were elucidated by X-ray diffraction (XRD, German Bruker D2) and scanning electron microscopy (SEM). Thermal parameters were measured through DSC with the temperature ranging from 50 °C to 400 °C at a heating rate of 10 °C/min by a TAQ2000 thermal analyzer. The visible to near-IR spectra were recorded using PerkinElmer Lambda 950 UV-Vis-NIR spectrophotometer. FTIR spectra were obtained using Nicolet 380 FTIR from 4000 cm^{-1} to 400 cm^{-1}. All optical tests were performed at room temperature.

3. Results and discussion

3.1 Amorphous nature analysis

The glass-forming ability of chalcogenide glass is usually evaluated by the amorphous state. Fig. 1 shows the typical XRD patterns of Ge–Ga–Te–Ag and Ge–Ga–Te–AgI glass samples. As presented in Fig. 1, there is no obvious crystallization peak in the curves. To ensure the absence of microcrystals in these glasses, a structural study using SEM was also performed to confirm the amorphous state. Fig. 2 shows that the surfaces of these glass samples are nearly homogeneous with no obvious microcrystals. All results indicate that Ge–Ga–Te–Ag and Ge–Ga–Te–AgI glass systems maintain their amorphous nature.

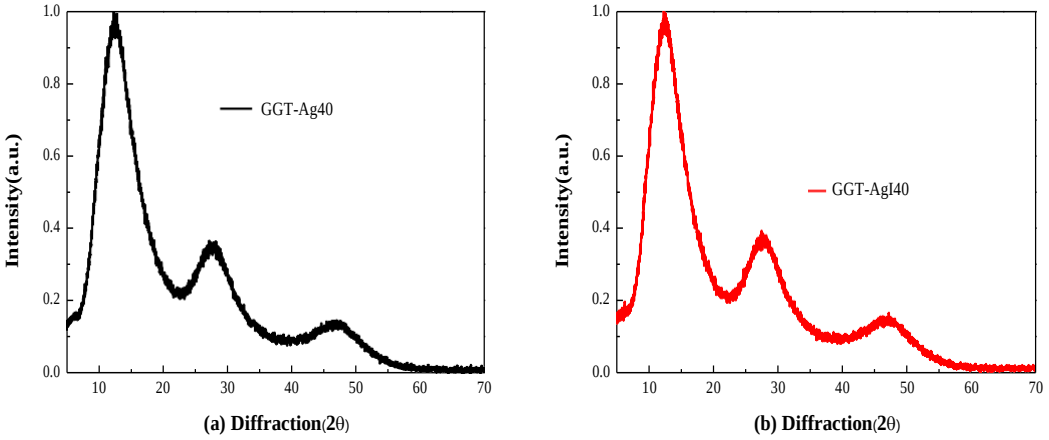

Fig. 1. XRD patterns of powder glass samples: (a) $(Ge_{15}Ga_{10}Te_{75})_{60}(Ag)_{40}$ and (b) $(Ge_{15}Ga_{10}Te_{75})_{60}(AgI)_{40}$.

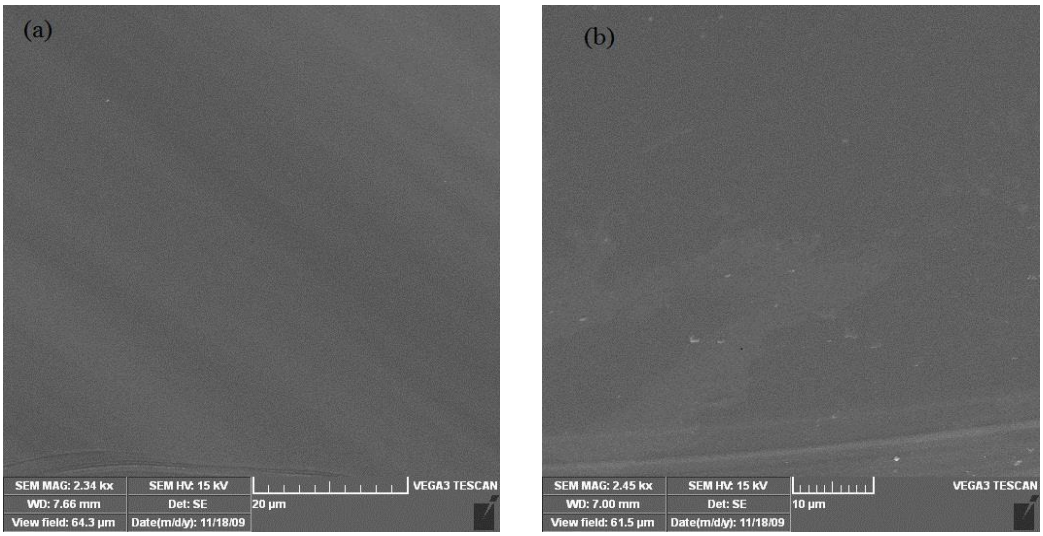

Fig. 2. SEM images of typical glass samples: (a) $(Ge_{15}Ga_{10}Te_{75})_{60}(Ag)_{40}$ and (b) $(Ge_{15}Ga_{10}Te_{75})_{60}(AgI)_{40}$.

3.2 Thermal properties analysis

The thermal parameters of these chalcogenide glasses were recorded using DSC instrument. Fig. 3 shows typical DSC curves of glass samples. T_g and glass onset crystallization temperature (T_x) can be obtained from these curves. Specific values are listed in Table 1. The T_g values of Ge–Ga–Te–Ag glasses are nearly the same with an increase of Ag content. However, the T_g value of Ge–Ga–Te–AgI glass increases with the addition of AgI. This behavior may be caused by silver atoms which locate at the end of long chains and form their own connected structure instead of opening the network of $GeTe_4$ tetrahedral or $GaTe_3$ triangle units. The bond energy of Te–Ag (9.46 kJ/mol) [15] is too small to influence the total bond energy of glasses. Therefore, the T_g values of Ge–Ga–Te–Ag glasses are almost the same. Given the chain-terminating function of I atoms, the addition of AgI opens up the network of $GeTe_4$ tetrahedral or $GaTe_3$ triangle units. Owing to its high electronegativity, I atoms capture the electrons from Te atoms. The bond energy of Te–I (198 kJ/mol) is larger than Ge–Te (171.3 kJ/mol) and Ga–Te (162.8 kJ/mol) bonds. The total bond energy of glass increases with an increase of AgI. As a result, the T_g value of Ge–Ga–Te–AgI glass increases gradually. The bond energy can be calculated using the following formula [16]:

$$D(A-B)=[D(A-A)*D(B-B)]^{0.5}+30(\chi_A-\chi_B)^2 \quad (1)$$

where, χ_A and χ_B are the electronegativity of the atoms A and B, respectively. $D(A–A)$ and $D(B–B)$ are the bond energy of A–A and B–B bonds, respectively. The values of chemical bond energy are shown in Table 2.

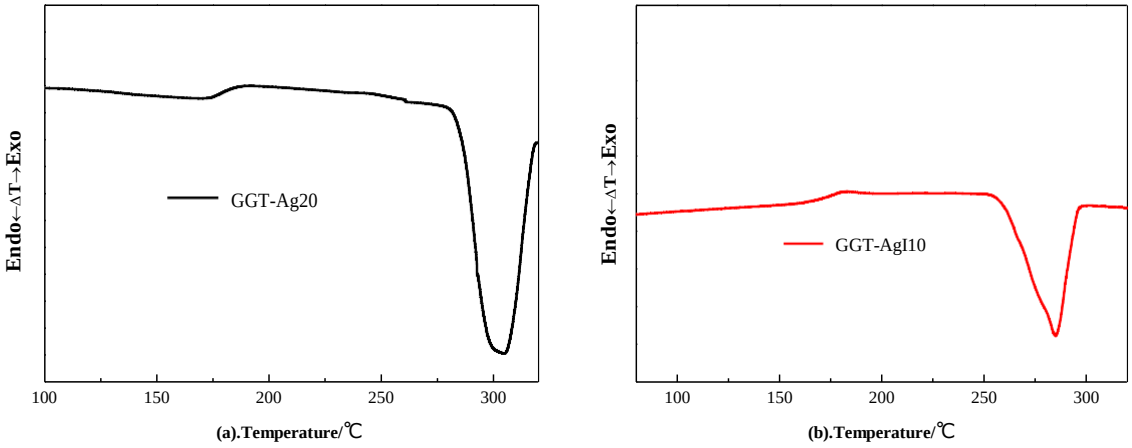

Fig. 3. DSC curves of typical glass samples: (a) $(Ge_{15}Ga_{10}Te_{75})_{80}(Ag)_{20}$ and (b) $(Ge_{15}Ga_{10}Te_{75})_{90}(AgI)_{10}$.

ΔT, the difference between T_x and T_g, is usually used to assess the thermal stability of chalcogenide glass. From Table 1, the largest ΔT values of Ge–Ga–Te–Ag and Ge–Ga–Te–AgI glasses are 110°C and 107°C, corresponding to $(Ge_{15}Ga_{10}Te_{75})_{80}(Ag)_{20}$ and $(Ge_{15}Ga_{10}Te_{75})_{90}(AgI)_{10}$ glass samples, respectively. As a whole, the thermal performance of Ge–Ga–Te–Ag glass system is superior to that of Ge–Ga–Te–AgI glass system.

Table 1

Thermal parameters of Ge–Ga–Te–Ag and Ge–Ga–Te–AgI glass samples.

Compositions	T_g/**°C**	T_x/**°C**	**ΔT/°C**
GGT–Ag10	176	284	108
GGT–Ag20	175	285	110
GGT–Ag30	175	280	105
GGT–Ag40	176	279	103
GGT–AgI10	152	259	107
GGT–AgI20	163	265	102
GGT–AgI30	166	263	97
GGT–AgI40	168	266	98

Table 2

Bond energy values of possible bonds.

Bond	Bond energy (kJ/mol)
Ge–Ge	163
Te–Te	235
Ge–Te	171
Ga–Te	163
Te–I	198
Ag–Te	9.46

3.3 IR spectra analysis

The IR optical transmission spectra of these glasses are shown in Fig. 4. All glass samples have wide IR windows, and the IR cut-off wavelengths reach above 25 μm. The transmittance sharply declines when the wavelength is beyond 20 μm. The reason may be the multi-phonon absorption produced by Ge–Te bond vibration [17]. With an increase of Ag or AgI, the transmittance of Ge–Ga–Te–Ag glass system deteriorates, whereas that of Ge–Ga–Te–AgI glass system ameliorates. The decrease of transmittance with an increase of Ag is attributed to the disorder caused by Ag atoms. Halide, as a modifier doping into Ge–Ga–Te glass, improves the anti-crystallization ability and the transmittance of Ge–Ga–Te–AgI glasses. Some absorption peaks can be observed in Fig. 4. The peak at 9.9 μm results from Si–O covalent bond vibration [9]. The peak at 15–20 μm is ascribed to the presence of oxygen contamination, such as Ge–O or Ga–O bond vibrations [7-18]. The intensity of absorption peak depends on the purity of the starting elements. To eliminate these absorption peaks aroused by oxide impurities, a distilling method with 400 ppm Mg was adopted. The IR spectra of purified glasses are shown in Fig. 5. With the help of Mg, the glasses have flat and wide IR optical transmission windows.

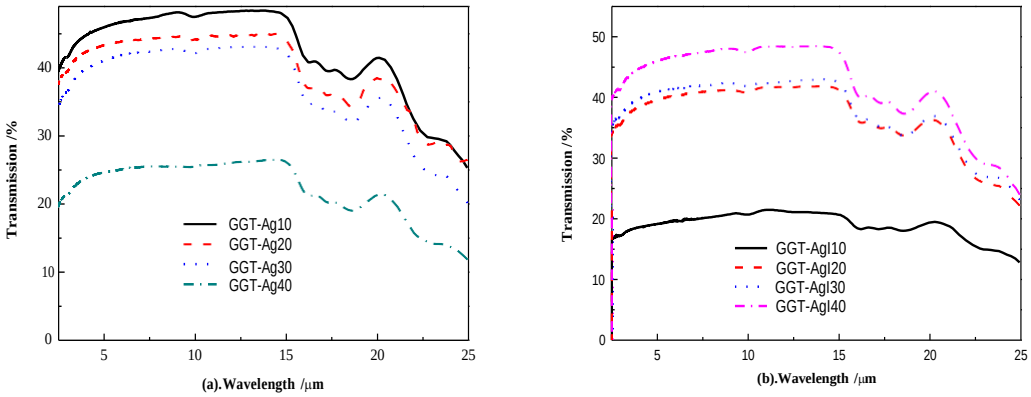

Fig. 4. IR transmission spectra of glass samples: (a) $(Ge_{15}Ga_{10}Te_{75})_{100-x}(Ag)_x$ and (b) $(Ge_{15}Ga_{10}Te_{75})_{100-x}(AgI)_x$

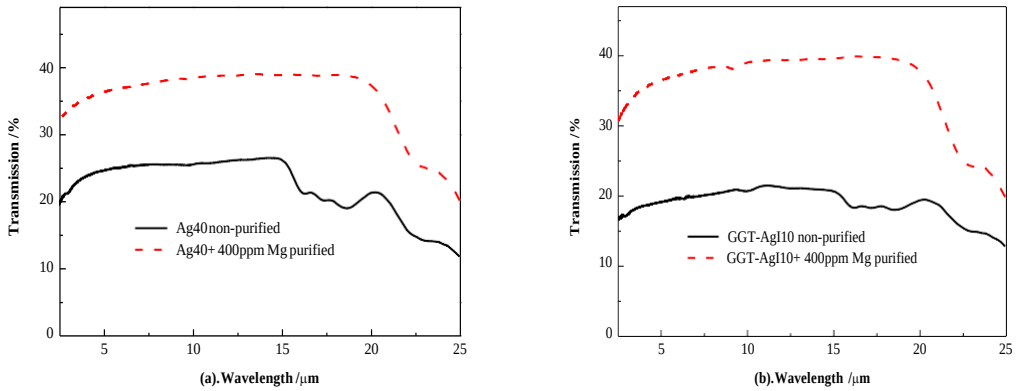

Fig. 5. IR spectra of purified glasses: (a). $(Ge_{15}Ga_{10}Te_{75})_{60}(Ag)_{40}$ and (b). $(Ge_{15}Ga_{10}Te_{75})_{90}(AgI)_{10}$.

3.4 Near-IR absorption spectra and optical band gap

The near-IR absorption spectra of Ge–Ga–Te–Ag and Ge–Ga–Te–AgI glasses are shown in Fig. 6. With an increase of Ag, the absorption cut-off edge of Ge–Ga–Te–Ag glass system shifts to the long wavelength region. On the contrary, the absorption cut-off edge of Ge–Ga–Te–AgI glass system shifts to the short wavelength region with an increase of AgI. These behaviors may be attributed to the high electronegativity of I atoms, which make the width of the forbidden band broader. Eventually, this results in the blue shift of the Ge–Ga–Te–AgI glass system. Elemental Ag and I show positive and negative effects on the glasses, respectively. Consequently, by combining two elements together, such as AgI, the effect on the glasses is determined by I atoms [19].

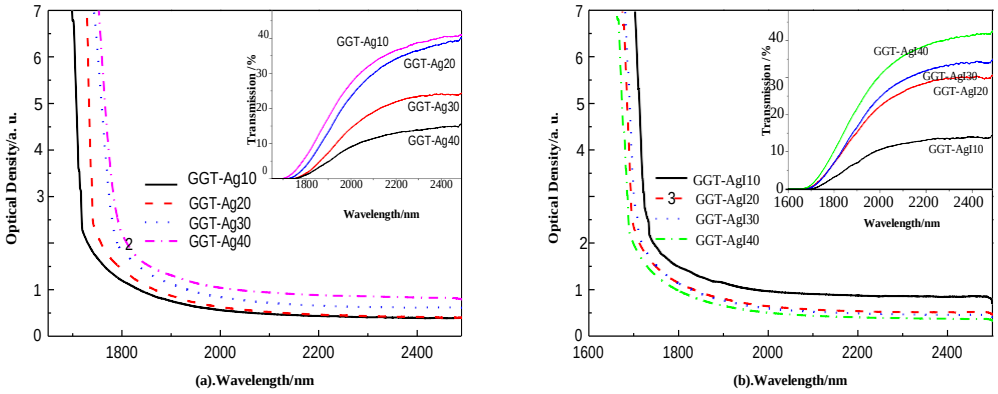

Fig. 6. Absorption spectra of glass samples. Inserts show the corresponding Vis-IR transmission spectra: (a) $(Ge_{15}Ga_{10}Te_{75})_{100-x}(Ag)_x$ and (b) $(Ge_{15}Ga_{10}Te_{75})_{100-x}(AgI)_x$.

The function relationship between absorption coefficient $\alpha(\omega)$ and optical band gap E_{opt} is given by Tauc equation [20]:

$$\alpha(\omega)\cdot\hbar\omega = B(\hbar\omega - E_{opt})^{m} \quad (2)$$

where α is the absorption coefficient, which is determined as α = 2.303 A/d (A is the optical density, d is the thickness of the glass sample), E_{opt} is the optical band gap, ħ is Plank constant, ω is the incident light angular frequency, and m is a parameter that can determine the transition type of absorption edge. For amorphous glass materials, the direct and indirect transitions correspond to m = 1/2 and m = 2, respectively. B is a constant about local state in the band gap. B can be calculated with the following equation:

$$B = \frac{(4\pi/c)\sigma_0}{n_0 \Delta E} \quad (3)$$

where c is the light speed in vacuum, σ_0 is the electrical conductivity under absolute zero, n_0 is the static refractive index, and ΔE is the local state tail width. Fig. 7 and Fig. 8 correspond to the direct and indirect band gaps of glasses, respectively. For Ge–Ga–Te–Ag glasses, E_{opt} decreases with an increase of Ag. However, an increase of AgI can broaden the optical band gap of Ge–Ga–Te–AgI glasses. Fig. 9 shows the tendency of E_{opt} of these glasses. In fact, the influence of Ag and I atoms on E_{opt} of glasses are totally opposite. The electrophilic character of I^- in Ge–Ga–Te–AgI glasses plays beneficial roles of trapping lone pair electrons from Te atoms, and exciting the electrons from filled to empty states. In chalcogenide glass material, the conduction band is formed by the empty orbits, whereas the valence band is formed by lone pair electrons. With an increase of AgI, the conduction band is hardly affected, but the valence band decreases.

Consequently, the optical band gap is broader and the effect of I supersedes that of Ag. E_{opt} decreases with an increase of Ag. This can be attributed to structural transformation. Ag atoms enter into the glass structure and forme their own connected structure [21]. In this constrained network structure, Ag causes an increase in disorder and decreases the optical band gap effectively. The values of optical band gap of all glass samples are listed in Table 3.

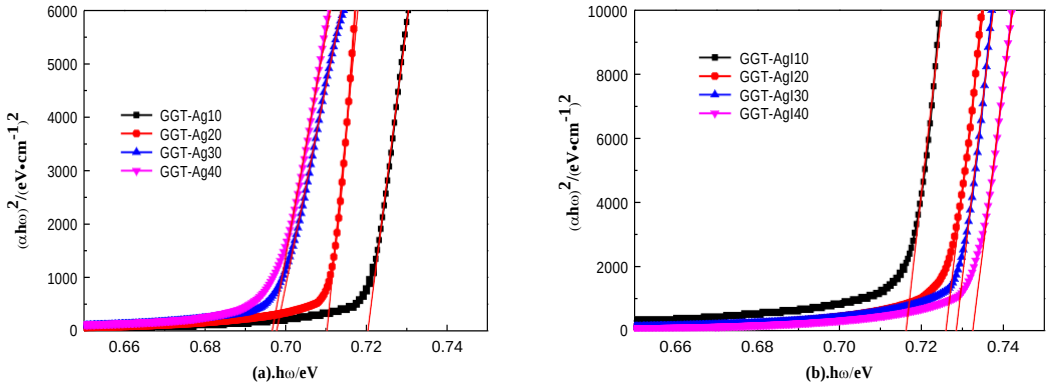

Fig. 7. Relationship between $(\alpha \bullet \hbar\omega)^2$ and $\hbar\omega$ for glass samples: (a) $(Ge_{15}Ga_{10}Te_{75})_{100-x}(Ag)_x$ and (b) $(Ge_{15}Ga_{10}Te_{75})_{100-x}(AgI)_x$.

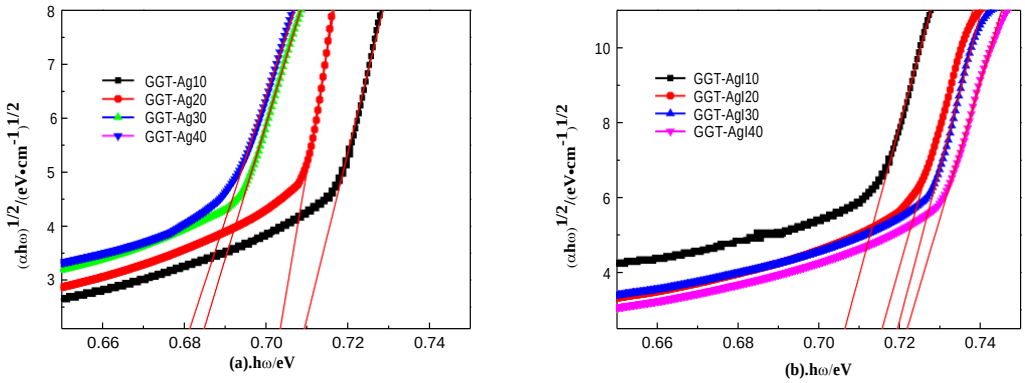

Fig. 8. Relationship between $(\alpha \bullet \hbar\omega)^{1/2}$ and $\hbar\omega$ for glass samples: (a) $(Ge_{15}Ga_{10}Te_{75})_{100-x}(Ag)_x$ and (b) $(Ge_{15}Ga_{10}Te_{75})_{100-x}(AgI)_x$.

Table 3

Optical band gap of Ge–Ga–Te–Ag and Ge–Ga–Te–AgI glasses.

Compositions	Thickness/cm	Direct-E_{opt}/(eV)	Indirect-E_{opt}/(eV)
GGT–Ag10	0.108	0.719	0.707
GGT–Ag20	0.104	0.709	0.702
GGT–Ag30	0.110	0.696	0.679
GGT–Ag40	0.105	0.695	0.675
GGT–AgI10	0.095	0.716	0.705
GGT–AgI20	0.104	0.725	0.715
GGT–AgI30	0.103	0.727	0.717
GGT–AgI40	0.103	0.731	0.719

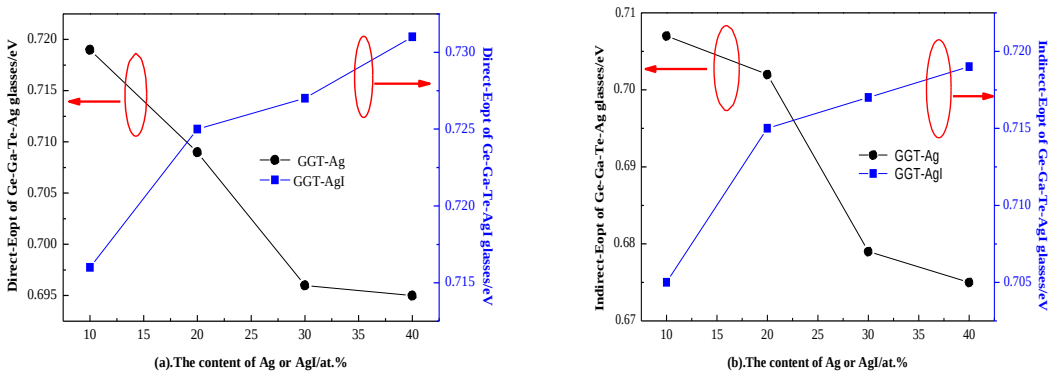

Fig. 9. Relationship between E_{opt} and the content of Ag or AgI: (a) Direct optical band gap and (b) Indirect optical band gap.

4. Conclusions

In this study, Ge–Ga–Te–Ag and Ge–Ga–Te–AgI glass systems were prepared and investigated. Results indicate that these glasses possess good amorphous state and thermal stability. An increase of Ag content results in a decrease in the optical band gap of Ge–Ga–Te–Ag glasses, whereas an increase of AgI content increases the optical band gap of Ge–Ga–Te–AgI glasses. The IR optical windows of these glasses are wide and flat, ranging from 1.8 μm to 20 μm. No obvious absorption peak exists after the purification method, which indicates that these glasses are promising material for far-IR applications.

Acknowledgment

This work was financially supported by the Natural Science Foundation of China (Grant Nos. 61435009, 61177087, and 61377099), National Program on Key Basic Research Project (973 Program) (Grant No. 2012CB722703), International Science & Technology Cooperation Program of China (Grant No. 2011DFA12040), Scientific Research Fund of Zhejiang Provincial Education Department (R1101263), Natural Science Foundation of Ningbo (Grant No. 2013A610118), Teaching and Research Award Program for Outstanding Young Teachers in Higher Education Institutions of MOE, P.R.C. Ningbo Optoelectronic Materials and Devices Creative Team (2009B21007), and Scientific Research Foundation of Graduate School of Ningbo University. This work was also sponsored by K. C. Wong Magna Fund of Ningbo University, the Outstanding (Postgraduate) Dissertation Growth Foundation of Ningbo University (Grant No. PY2014014), and the Scientific Research Foundation of Graduate School of Ningbo University.

References

[1] X. Zhang, G. Fonteneau, J. Lucas, Tellurium halide glasses. New materials for transmission in the 8–12 μm range, J. Non-Cryst. Solids 104 (1988) 38-44.

[2] J. Lucas, X. Zhang, The tellurium halide glasses, J. Non-Cryst. Solids 125 (1990) 1-16.

[3] S. Danto, P. Houizot, C. Boussard‐Pledel, A Family of Far‐Infrared‐Transmitting Glasses in the Ga–Ge–Te System for Space Applications, Adv. Funct. Mater. 16 (2006) 1847-1852.

[4] G.R. Elliott, D.W. Hewak, G.S. Murugan, Chalcogenide glass microspheres; their production, characterization and potential, Opt. Express 15 (2007) 17542-17553.

[5] A.A. Wilhelm, C. Boussard‐Pledel, Q. Coulombier, Development of Far‐Infrared‐Transmitting Te Based Glasses Suitable for Carbon Dioxide Detection and Space Optics, Adv. Mater. 19 (2007) 3796-3800.

[6] S. Maurugeon, B. Bureau, C. Boussard-Plédel, Te-rich Ge–Te–Se glass for the CO_2 infrared detection at 15μm, J. Non-Cryst. Solids 355 (2009) 2074-2078.

[7] S. Sen, E. Gjersing, B. Aitken Physical properties of $Ge_xAs_{2x}Te_{100-3x}$ glasses and Raman spectroscopic analysis of their short-range structure, J. Non-Cryst. Solids 356 (2010) 2083-2088.

[8] X. Wang, Q. Nie, G. Wang, Investigations of Ge–Te–AgI chalcogenide glass for far-infrared application, Spectrochimica Acta Part A: Molecular and Biomolecular Spectroscopy 86 (2012) 586-589.

[9] C. Cheng, X. Wang, T. Xu, Novel Ge–Ga–Te–CsBr glass system with ultrahigh resolvability of halide, Spectrochimica Acta Part A: Molecular and Biomolecular Spectroscopy 150 (2015) 737-741.

[10] S. Cui, C. Boussard-Plédel, J. Lucas, Te-based glass fiber for far-infrared biochemical sensing up to 16 μm, Opt. Express 22 (2014) 21253-21262.

[11] Y. He, X. Wang, Q. Nie, Optical properties of Ge–Te–Ga doping Al and $AlCl_3$ far infrared transmitting chalcogenide glasses, Infrared Physics & Technology 58 (2013) 1-4.

[12] S. Maurugeon, B. Bureau, C. Boussard-Plédel, Te-rich Ge–Te–Se glass for the CO_2 infrared detection at 15μm, J. Non-Cryst. Solids 355 (2009) 2074-2078.

[13] K. Ramesh, S. Asokan, K. Sangunni, Glass formation in germanium telluride glasses containing metallic additives, J. Phys. Chem. Solids 61 (2000) 95-101.

[14] J. Sun, Q. Nie, X. Wang, Glass formation and properties of Ge–Te–BiI_3 far infrared transmitting chalcohalide glasses, Spectrochimica Acta Part A: Molecular and Biomolecular Spectroscopy 79 (2011) 904-908.

[15] Q. Nie, G. Wang, X. Wang, Glass formation and properties of $GeTe_4$–Ga_2 Te_3–AgX (X= I/Br/Cl) far infrared transmitting chalcohalide glasses, Optics Communications 283 (2010) 4004-4007.

[16] L. Pauling, *The Nature of Chemical Bonds*. (Cornell University, New York, 1960), p.175.

[17] C. Quémard, F. Smektala, V. Couderc, Chalcogenide glasses with high non linear optical properties for telecommunications, J. Phys. Chem. Solids 62 (2001) 1435-1440.

[18] K.S. Andrikopoulos, S.N. Yannopoulos, A.V. Kolobov, Raman scattering study of GeTe and $Ge_2Sb_2Te_5$ phase-change materials, J. Phys. Chem. Solids 68 (2007) 1074-1078.

[19] S. Cui, D. Le Coq, C. Boussard-Plédel, Electrical and optical investigations in Te–Ge–Ag and Te–Ge–AgI chalcogenide glasses, J. Alloys Compd. 639 (2015) 173-179.

[20] A. Kolobov, P. Fons, J. Tominaga, Crystallization-induced short-range order changes in amorphous GeTe, J. Phys.: Condens. Matter 16 (2004) S5103.

[21] M. Sakurai, F. Kakinuma, E. Matsubara, Partial structure analysis of amorphous $Ge_{15}Te_{80}M_5$ (M= Cu, Ag and In), J. Non-Cryst. Solids 312 (2002) 585-588.